

## Direct Observation of Localized Second-Harmonic Enhancement in Random Metal Nanostructures

Sergey I. Bozhevolnyi,<sup>1,\*</sup> Jonas Beermann,<sup>1</sup> and Victor Coello<sup>2</sup>

<sup>1</sup>*Institute of Physics, Aalborg University, Pontoppidanstræde 103, DK-9220 Aalborg Øst, Denmark*

<sup>2</sup>*CICESE Monterrey, Pedro de Alba S/N Edificio de Posgrado FCFM-Uanl, C. P. 66450 S. N. de los Garza N. L., Mexico*

(Received 7 February 2003; published 15 May 2003)

Second harmonic (SH) scanning optical microscopy in reflection is used to image the gold film surface covered with randomly placed scatterers. SH images obtained with a tightly focused tunable (750–830 nm) laser beam show small ( $\sim 0.7 \mu\text{m}$ ) and very bright ( $\sim 10^3$  times the background) spots, whose locations depend on the wavelength and polarization of light. Comparing SH and fundamental harmonic (FH) images, we conclude that the localized SH enhancement occurs due to the overlap of FH and SH eigenmodes. The probability density function of the SH signal is found to follow the power-law dependence.

DOI: 10.1103/PhysRevLett.90.197403

PACS numbers: 78.67.Bf, 42.65.Ky, 73.20.Mf, 81.07.–b

Light-matter interactions in nanostructured materials give rise to nanostructured optical fields whose distinctive properties bring about various fascinating phenomena, including light localization, photonic band gap effect, and surface enhanced scattering [1,2]. Profound understanding of fundamental and applied aspects of these phenomena is crucial for further progress in nanoscience and nanotechnology. Strong (up to several orders of magnitude) and spatially localized (on nanometer scale) field intensity enhancement is one of the most remarkable effects in light scattering by *metal* nanostructures that plays a major role in surface enhanced phenomena, e.g., Raman scattering and second-harmonic (SH) generation. In the system of noninteracting (rarely spaced) scatterers, the enhancement is due to the lightning rod effect (at sharp angled surfaces) and shape-dependent resonant oscillations of the electrons, i.e., localized surface plasmons (SPs) [3]. The first effect being the effect of single scattering is only weakly wavelength dependent, whereas the second one is related to multiple scattering (inside an individual particle) leading to a discrete set of resonance frequencies determined by the particle's shape and its dielectric constant. In the system of strongly interacting random nanoparticles, resonant SP excitations (eigenmodes of the system) tend to be localized in nm-sized volumes with resonance frequencies covering a wide spectrum range from near UV to far IR [4]. Here the field enhancement is due to multiple interparticle light scattering, and the resonant eigenmodes exhibit very different strength, phase, polarization, and localization characteristics. Their existence is well documented in the experiments on near-field imaging of disordered metal nanostructures [5]. Note that these experiments dealt with *linear* scattering, i.e., localized intensity enhancement has been observed at the frequency of the illumination.

Enhanced SH generation at rough metal surfaces has been a subject of numerous experimental and theoretical investigations concerned mainly with the angular distri-

bution of far-field SH radiation [6]. Spatially resolved SH measurements at rough metal surfaces conducted with a near-field microscope have been also reported [7,8] with the observed local SH enhancement being ascribed to the SP localization [7] or lightning rod effect [8]. However, bright regions seen in the SH images obtained in the first case were rather diffuse and noisy, and the suggested origin (localization) was not corroborated with, e.g., wavelength-dependent measurements. Quite recently, strongly enhanced SH generation characterized by a broad angular (far-field) distribution has been observed with gold-glass films near the percolation threshold [9]. A large diffuse SH component indicates (though *indirectly*) the occurrence of localized SPs that generate strongly fluctuating (in amplitude, phase, and polarization) local SH sources.

In this Letter, we report what we believe to be the first *direct* observations of strong and spatially localized SH enhancement in random metal nanostructures that exhibits sensitivity with respect to the wavelength and polarization of light. The sample used in this work has been prepared by evaporating a 55-nm-thick gold film on a glass substrate and covering the film surface with areas filled with randomly located 70-nm-high gold bumps (nominal density was  $50 \mu\text{m}^{-2}$ ). A standard fabrication procedure based on electron-beam lithography, gold evaporation and liftoff has been employed resulting in the structures similar to those used for the demonstration of SP polariton localization and waveguiding in random nanostructures [10]. Because of proximity effects in the exposure, the final structures contained not only random individual bumps (50–100 nm in diameter) but also larger islands formed of their clusters (Fig. 1).

The experimental setup for SH microscopy was essentially the same as that used in the experiments with semiconductor microstructures [11]. It consists of a scanning optical microscope in reflection geometry built on the base of a commercial microscope and a

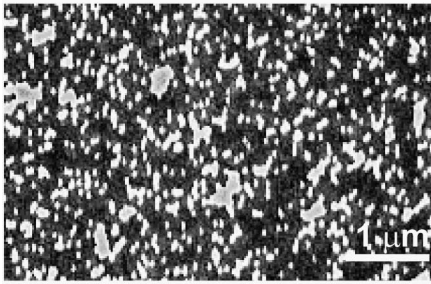


FIG. 1. Scanning electron microscope image of a scattering region composed of random individual gold bumps and clusters with a nominal density of  $50 \mu\text{m}^{-2}$ .

computer-controlled two-dimensional piezoelectric translation stage (steps down to 50 nm, accuracy  $\sim 4$  nm). The linearly polarized light beam from a mode-locked pulsed (pulse duration  $\sim 200$  fs, repetition rate  $\sim 80$  MHz) Ti:sapphire laser ( $\lambda = 750\text{--}830$  nm,  $\delta\lambda \sim 10$  nm, average power 300 mW) used as a source of sample illumination at the fundamental harmonic (FH) frequency. After passing an optical isolator (to avoid back reflection), half-wave plate, polarizer, and wavelength selective beam splitter, the laser beam is focused on the sample surface at normal incidence with a Mitutoyo infinity-corrected  $\times 100$  objective (spot size  $\approx 1 \mu\text{m}$ ). The illumination power was kept at the level of  $\sim 20$  mW (intensity at the surface  $\sim 2 \times 10^6$  W/cm $^2$ ) to avoid thermal damage of the sample surface. The SH radiation generated in reflection and the reflected FH beam are collected with the same objective, separated by the beam splitter, directed through the appropriate filters and polarizers and detected with a photomultiplier tube (connected with a photon counter) and a photodiode, respectively. Both SH and FH signals are simultaneously recorded as a function of the scanning coordinate resulting in the SH and FH images of the sample surface. During a normal scan, the SH photons at each point are counted over a period of 20 ms with four dark counts on average, i.e., 200 cps or 0.2 kcps. Using this setup to image thin ( $< 100$  nm) domain walls in ferroelectric crystals fabricated for quasiphase matched SH generation [12], we have evaluated the resolution in the SH images as being  $\approx 0.7 \mu\text{m}$ . This value is consistent with the aforementioned FH spot size determined from the FH images of test structures, since the SH intensity scales quadratically with the FH one.

Typical FH and SH images obtained with the scattering region (Fig. 1) for different FH wavelengths are shown in Fig. 2. The FH images showed low contrast with the signal varying in the range of  $(0.9\text{--}1.2)S_0$ , where  $S_0$  is the signal measured at the flat gold film surface. They feature well-pronounced dark spots whose contrast is wavelength dependent (see the evolution of spots A and B in Fig. 2). One can also distinguish rather weak bright spots with wavelength-dependent contrast. In order to

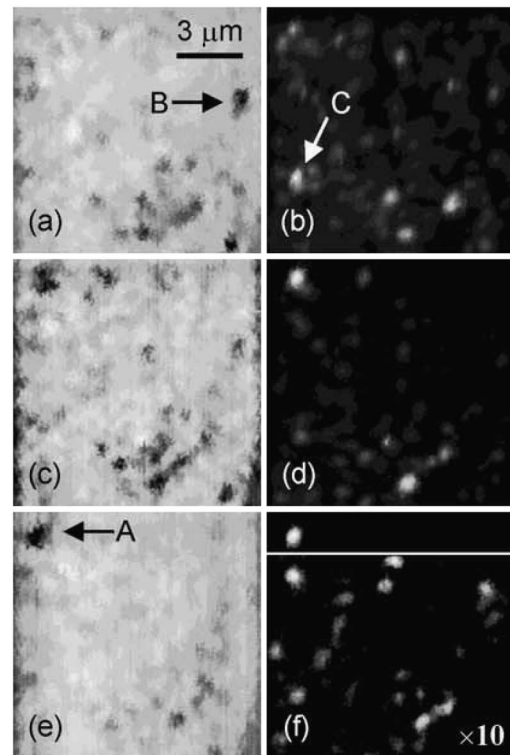


FIG. 2. Gray-scale (a),(c),(e) FH and (b),(d),(f) SH images ( $11.5 \times 11.5 \mu\text{m}^2$ ) of the random structure taken at the FH wavelength  $\lambda \equiv$  (a),(b) 750, (c),(d) 790, and (e),(f) 830 nm. The polarization of the incident FH and detected SH radiation was vertical with respect to the presented images. The maximum of the SH signal corresponds to (b) 325, (d) 120, and (f) 145 kcps.

account for these observations, let us consider the reflected FH radiation as a superposition of the FH beam reflected from the flat gold surface and the FH field scattered by strongly interacting gold bumps (strong interaction via SP polaritons has been found in a similar system [10]). The latter contribution can be associated with the excitation of luminous FH eigenmodes (of the scattering system) that couple efficiently to far-field radiation [13]. These modes are very different in their characteristics, and probably several modes can be excited simultaneously since, on average, there are  $\sim 50$  scatterers within the FH beam spot. However, we expect the most efficient excitation for well-localized modes with one strong field maximum. Light scattering via excitation of such a mode should be similar to the dipole scattering resulting in the excitation of SP polariton modes (being in turn scattered in the surface plane and into the substrate as well as absorbed due to the internal damping). These processes contribute to the decrease of the total flux in the direction of reflection and, thereby, formation of dark spots. On the other hand, the FH spot size ( $\approx 1 \mu\text{m}$ ) is very large in comparison with the typical mode localization radius, which is on nanometer

scale. One can expect simultaneous excitation of different modes and their combined influence on the detected FH signal is difficult to predict. The above circumstances lead to overall weak contrast in the FH images because of averaging effects (small mode sizes, different modes) and background FH reflection from the flat film surface.

This background is practically absent in the SH images because the SH signal from the flat surface was  $\sim 0.5$  kcps, i.e., only 2.5 times larger than the average SH noise level. The SH images exhibited diffraction-limited (size  $\sim 0.7 \mu\text{m}$ ) and very bright (up to 500 kcps) spots, whose brightness and locations depended on the wavelength [cf. Figs. 2(b), 2(d), and 2(f)]. Comparing the FH and SH images we noticed that, quite often, bright SH spots coincided with dark FH spots, although the SH signal could be rather different for similar dark spots (cf. SH signals for spots *A* and *B* in Fig. 2). In fact, bright SH spots could also be found at local FH maxima or even at places showing monotonous variations in the FH signal [e.g., SH spot *C* in Fig. 2(b)]. These features suggest the following explanation. Excitation of an FH eigenmode (leading to the local FH enhancement) results in a strong SH signal *only* if the SH field, which is associated with the generated nonlinear polarization, is *further* enhanced due to excitation of the corresponding SH eigenmode. This means that the FH and SH eigenmodes should *overlap* in the surface plane. Since the effect of simultaneous excitation of different FH eigenmodes on the FH signal is rather intricate, it should not be expected to find strong correlation between FH and SH images. However, since dark wavelength-dependent FH spots are definitely due to the excitation of at least one strong FH eigenmode, it is expected that at least *some* of the dark FH spots coincide with the bright SH spots.

The polarization characteristics of these modes are also important. Different polarizations of the incident FH radiation lead to the excitation of different FH eigenmodes (since different eigenmodes possess different polarization properties) that in turn efficiently overlap with different SH eigenmodes. Indeed, we observed that the change in the polarization of the FH incident beam resulted in the modification of both FH [cf. Figs. 3(a) and 3(c)] and SH images [cf. Figs. 2(b) and 3(d)]. Bearing in mind that the polarization is not preserved in the regime of multiple scattering, it is expected that the polarization of an excited SH eigenmode can differ from that of the incident FH field, depending on the polarization of the *total* (self-consistent) FH field at the particular place. We have observed that the signal level was the same for the detected SH radiation being polarized parallel and perpendicular to that of the incident FH beam, but the SH images were rather different [cf. Figures 2(b) and 3(b)]. The observed polarization sensitivity is apparently consistent with the explanation suggested above for the formation of FH and SH images. In fact, the overlap (in location and polarization) condition for localized modes

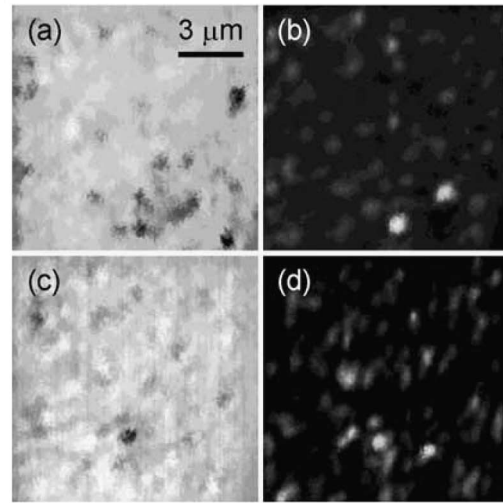


FIG. 3. Gray-scale (a),(c) FH and (b),(d) SH images ( $11.5 \times 11.5 \mu\text{m}^2$ ) of the same area as imaged in Fig. 2 [Figs. 2(a) and 3(a) are the same] taken at the FH wavelength  $\lambda \cong 750$  nm for different polarization orientations: (a) FH vertical together with (b) SH horizontal, and (c) FH horizontal together with (d) SH vertical. The maximum of the SH signal corresponds to (b) 110 and (d) 115 kcps.

can be perceived as an analog to the phase matching condition for propagating waves. Indeed, the coexistence of the FH and SH eigenmodes means that the SH field driven by the FH eigenmode is *in phase* with multiply scattered SH fields (that actually form the SH eigenmode).

The SH bright spots being similar in appearance (round and diffraction limited in size) were found to have very different maximum signals: from 1 to 500 kcps. For example, the bright SH spot corresponding to spot *A* in Fig. 2 completely dominates the SH image taken at  $\lambda_{FH} = 830$  nm, so that other spots are seen only when enhanced by 10 times [Fig. 2(f)]. We explain the observed giant fluctuations in the maximum SH signal by the circumstance that, within the FH beam spot, there can happen only one event (if at all) of sufficient overlap of FH and SH modes. To some extent, the excited FH mode can be considered as a local probe of the corresponding SH mode. In linear near-field probing of the localized field enhancement, it has been found useful to evaluate the probability distribution function (PDF) for the local field intensities that provides a quantitative estimate of the intensity changes over the sample area [14]. In our case, the PDF of SH signal enhancement (with respect to the SH signal from flat surface regions) was found to follow the power-law dependence for large signals (Fig. 4), a feature that is actually expected for self-similar (e.g., fractal) clusters of nanoparticles [15]. Leveling off of the obtained PDFs (for large SH signal enhancements) is believed to relate to the usage of a limited data set, i.e., to finite statistics effects. Treating

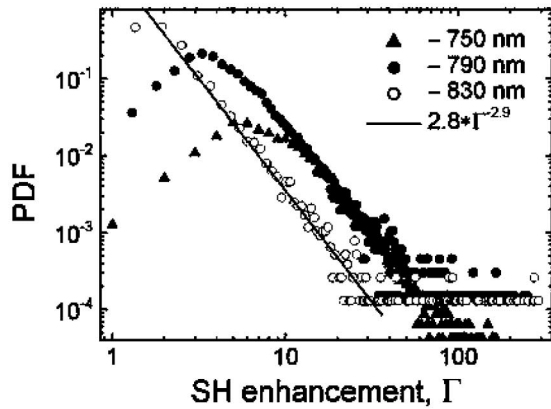


FIG. 4. The PDF calculated from the SH signal data (normalized by the signal from flat regions) shown in the images of Fig. 2 along with the power-law fit (solid line) for the data obtained with the FH wavelength of 830 nm. Each PDF was calculated from the 13225 image data points dividing the interval between the maximum and minimum signals by 500 sampling intervals.

$\sim 30$  similar (in size) SH images obtained with different wavelengths, polarization configurations, and surface regions (sampled from the area of  $25 \times 25 \mu\text{m}^2$ ), we obtained somewhat different powers of the PDF tails (from  $-2.4$  to  $-3.4$ ) centered at the power of  $-2.8$ . It is interesting to note that this power is  $\sim 2$  times larger than the universal index ( $-1.5$ ) simulated for the PDF of linear intensity enhancement [15]. At the same time, the PDF determined in linear near-field experiments decreased exponentially [14]. These facts are yet to be properly explained, though one might suggest that the required overlap of nm-sized FH and SH eigenmodes decreases the influence of averaging effects on the PDF [14] and their nonlinear interaction results in a steeper power-law dependence than that expected for *linear* scattering [15].

In summary, using SH scanning optical microscopy in reflection we have imaged the 55-nm-thick gold film surface covered with randomly 70-nm-high gold bumps (nominal density  $\sim 50 \mu\text{m}^{-2}$ ). It has been found that the FH and SH images obtained with a tightly focused (spot size  $\approx 1 \mu\text{m}$ ) tunable (750–830 nm) laser beam show wavelength and polarization dependent contrast. The contrast in FH images was rather weak, while the SH images exhibited small ( $\sim 0.7 \mu\text{m}$ ) and very bright ( $\sim 10^3$  times the background) spots. These features have been attributed to the excitation of resonant eigenmodes that are expected to exist in a system of (strongly interacting) metal nanoparticles. Furthermore, comparing the SH and FH images, we have concluded that the localized SH enhancement occurs due to overlap (in location and polarization) of the FH and SH eigenmodes. The fact that

the PDF of the SH signal was found to follow the power-law dependence supports also this conclusion. Overall, the results obtained constitute a *direct* evidence of intense nm-sized fields of resonant eigenmodes (localized SPs) generated via *nonlinear* interactions in metal nanostructures and highlight the important requirement of overlap needed for their efficient generation. The latter circumstance is very important and should be borne in mind when studying surface enhanced nonlinear scattering phenomena such as nonlinear optical probing and nano-modification.

The authors thank K. Leosson and A. Boltasseva for the fabrication and scanning electron microscopy characterization of the sample used in this work.

\*Corresponding author.

Email address: sergey@physics.auc.dk

- [1] *Optics of Nanostructured Materials*, edited by V.M. Markel and T.F. George (Wiley, New York, 2001).
- [2] *Optical Properties of Nanostructured Random Media*, edited by V.M. Shalaev (Springer-Verlag, Berlin, 2002).
- [3] G.T. Boyd, Th. Rasing, J.R.R. Leite, and Y.R. Shen, *Phys. Rev. B* **30**, 519 (1984), and references therein.
- [4] A.K. Sarychev and V.M. Shalaev, *Phys. Rep.* **335**, 275 (2000); M.I. Stockman, in *Optics of Nanostructured Materials* [1], p. 313, and references therein.
- [5] D.P. Tsai *et al.*, *Phys. Rev. Lett.* **72**, 4149 (1994); S.I. Bozhevolnyi, I.I. Smolyaninov, and A.V. Zayats, *Phys. Rev. B* **51**, 17916 (1995); P. Zhang, T.L. Haslett, C. Douketis, and M. Moskovits, *ibid.* **57**, 15513 (1998); S.I. Bozhevolnyi and V. Coello, *ibid.* **58**, 10899 (1998); V.A. Markel *et al.*, *ibid.* **59**, 10903 (1999); S. Gréillon *et al.*, *Phys. Rev. Lett.* **82**, 4520 (1999).
- [6] T.A. Leskova, A.A. Maradudin, and E.R. Méndez, in *Optical Properties of Nanostructured Random Media* [2], p. 359, and references therein.
- [7] I.I. Smolyaninov, A.V. Zayats, and C.C. Davis, *Phys. Rev. B* **56**, 9290 (1997).
- [8] A.V. Zayats, T. Kalkbrenner, V. Sandoghdar, and J. Mlynek, *Phys. Rev. B* **61**, 4545 (2000).
- [9] M. Breit *et al.*, *Phys. Rev. B* **64**, 125106 (2001).
- [10] S.I. Bozhevolnyi, V.S. Volkov, and K. Leosson, *Phys. Rev. Lett.* **89**, 186801 (2002).
- [11] S.I. Bozhevolnyi, A. Mailykovski, B. Vohnsen, and V. Zwiller, *J. Appl. Phys.* **90**, 6357 (2001).
- [12] B. Vohnsen and S.I. Bozhevolnyi, *J. Microsc.* **202**, 244 (2001).
- [13] M.I. Stockman, S.V. Faleev, and D.J. Bergman, *Phys. Rev. Lett.* **87**, 167401 (2001).
- [14] S.I. Bozhevolnyi and V. Coello, *Phys. Rev. B* **64**, 115414 (2001); K. Seal *et al.*, *ibid.* **67**, 035318 (2003).
- [15] M.I. Stockman, L.N. Pandey, L.S. Muratov, and T.F. George, *Phys. Rev. Lett.* **72**, 2486 (1994).